

The long non-coding RNA BDNF-AS induces neuronal cell apoptosis by targeting miR-125b-5p in Alzheimer's disease models

*Haiyan Ren^{1,A–F}, *Weibin Qiu^{2,A–F}, Benju Zhu^{1,B,C,F}, Qiang Li^{1,B,C,F}, Chen Peng^{1,B,C,F}, Xu Chen^{1,E,F}

¹ Department of Neurology, Shanghai Eighth People's Hospital, China

² Department of Neurology, Shanghai Xuhui Central Hospital, China

A – research concept and design; B – collection and/or assembly of data; C – data analysis and interpretation;

D – writing the article; E – critical revision of the article; F – final approval of the article

Advances in Clinical and Experimental Medicine, ISSN 1899–5276 (print), ISSN 2451–2680 (online)

Adv Clin Exp Med. 2024;33(3):233–245

Address for correspondence

Xu Chen

E-mail: hbpetrel@163.com

Funding sources

This study was funded by Jiangsu University Clinical Medical Science and Technology Development Fund Project (grant No. JLY2021104).

Conflict of interest

None declared

*Haiyan Ren and Weibin Qiu contributed equally to this work.

Received on September 28, 2022

Reviewed on February 3, 2023

Accepted on June 12, 2023

Published online on July 24, 2023

Cite as

Ren H, Qiu W, Zhu B, Li Q, Peng C, Chen X. The long non-coding RNA BDNF-AS induces neuronal cell apoptosis by targeting miR-125b-5p in Alzheimer's disease models. *Adv Clin Exp Med*. 2024;33(3):233–245. doi:10.17219/acem/168241

DOI

10.17219/acem/168241

Copyright

Copyright by Author(s)

This is an article distributed under the terms of the Creative Commons Attribution 3.0 Unported (CC BY 3.0) (<https://creativecommons.org/licenses/by/3.0/>)

Abstract

Background. At least 55 million individuals suffer from dementia globally, of which Alzheimer's disease (AD) accounts for 60–70% of cases. Alzheimer's disease is the only major cause of death that is still growing. However, the molecular mechanisms are largely unknown in the progress of AD.

Objectives. The goal of the study was to assess whether lncRNA brain-derived neurotrophic factor antisense (BDNF-AS) could affect processes underlying the regulation of neuronal cell apoptosis in rat and cellular models of AD by directing the expression of miR-125b-5p.

Materials and methods. The amyloid- β ($A\beta$)_{1–42}-induced rat and cellular models of AD were established. Changes in learning and memory in rats were detected with the use of the Morris water maze. Cell viability and apoptosis were determined using the 3-(4,5-dimethylthiazol-2-yl)-2,5 diphenyl tetrazolium bromide (MTT) test and flow cytometry. Reverse transcription-quantitative polymerase chain reaction (RT-qPCR) was applied to detect the expression of lncRNA BDNF-AS and miR-125b-5p, and western blotting was utilized to examine proteins. The correlations between lncRNA BDNF-AS and miR-125b-5p were demonstrated using dual-luciferase reporter gene assays.

Results. Our results showed that BDNF-AS was upregulated and miR-125b-5p was downregulated in the rat and cellular AD models. The addition of si-BDNF-AS and miR-125b-5p mimics shortened the escape latency and swimming distance in the rat model. Furthermore, the knockdown of BDNF-AS or the administration of miR-125b-5p mimic significantly suppressed cell apoptosis, cell inflammatory, and inflammatory pathway-related proteins, while these cellular activities were promoted in rat and cellular models of AD. Additionally, miR-125b-5p was found to be a BDNF-AS target gene that was linked negatively with BDNF-AS in AD.

Conclusions. Through regulation of miR-125b-5p, lncRNA BDNF-AS suppressed cell death, inflammation and inflammatory pathway-related proteins in AD models, which provides a potential biomarker and therapeutic target in the clinical treatment of AD.

Key words: lncRNA BDNF-AS, miR-125b-5p, $A\beta$ _{1–42}, apoptosis, Alzheimer's disease

Background

Alzheimer's disease (AD) is a common neurodegenerative disease that results in progressive memory loss, neurocognitive dysfunction, and personality and behavioral changes that have a significant impact on disability-adjusted life years.^{1,2} Neurodegeneration, the main pathological feature of AD, is an irreversible and incurable process in which neurons gradually atrophy and lose function in specific parts of the brain, eventually leading to neuron death.^{3–5} Neuronal injury and death disrupt the connections between neuronal networks, causing multiple brain regions to atrophy. In AD patients, the atrophy of the hippocampal and medial temporal lobe areas is the structural feature detected with magnetic resonance imaging (MRI).⁶

Histopathologically, the progressive neurodegenerative disorder is distinguished by amyloid- β (A β) peptide and tau.^{7,8} The toxic A β aggregates and assembles into extracellular amyloid plaques that are deposited in specific areas of the brain and cause a reduction in synapses.^{9,10} This occurs first in the temporal cortex region, containing the hippocampus, which is implicated in the formation of memories.^{8,11} The neuronal toxicity of A β manifests itself by binding to a variety of receptors, including $\alpha 7$ nicotinic acetylcholine receptor ($\alpha 7$ nAChR), p75 neurotrophin receptor (p75NRT) and N-methyl-D-aspartate receptor (NMDAR).^{12,13} The interactions between A β and these receptors have been proposed to cause hyperphosphorylation of tau, endoplasmic reticulum (ER) stress responses, mitochondrial dysfunction and inflammatory responses, and, ultimately, lead to synaptic dysfunction and neuronal death.^{14,15} Hyperphosphorylated tau constitutes neurofibrillary tangles (NFTs) that can initiate the disassembly of microtubules in the medial temporal lobe, thereby playing a significant role in episodic memory function.^{14,16,17} At the same time, the cytotoxicity of tau can lead to synaptic dysfunction and neuronal cell cycle re-entry.^{7,18} Many studies focusing on A β and tau have had limited success, indicating that the late timing of intervention and focus on a single target are insufficient to block the cascade responses in the neural network system.

MicroRNAs (miRNAs) are a class of small non-coding RNAs that play an important role in regulating the post-transcriptional expression of target genes.¹⁹ Circulating miRNAs are easily detectable and highly stable; thus, many studies have investigated circulating miRNAs in human body fluids such as serum, breast milk, saliva, bile, and urine.^{20,21} In recent years, many studies have confirmed the relevance of the aberrant expression of miRNAs in a variety of diseases, such as cardiovascular disease (CVD), diabetes, tumors, and neurodegenerative diseases.²² Both the type and expression pattern of miRNAs can be used as indicators of the type, progression and pathology of disease.^{23,24} For example, overexpressed miR-124 causes hyperphosphorylation of insoluble tau protein by targeting PTPN1, while the tau protein shifts from axon

to dendrite, resulting in AD-like tau pathology.²⁵ Furthermore, upregulated miR-146a promotes M2 polarization of microglia stimulated by inflammation, inhibits the secretion of inflammatory factors, and enhances the phagocytotic capacity.²⁶ The miR-24-3p/STING pathway can reduce neuroinflammation caused by excessive A β deposition in the brains of patients with AD.²⁷ MicroRNA-125b has an irreplaceable role in many intracellular activities or pathological states, but its effect on AD is, to date, rather controversial.

Long non-coding RNAs (lncRNAs) play a significant role in neurodegenerative illnesses such as AD, Parkinson's disease (PD) and Huntington's disease (HD). Similar to AD, the death of dopamine-secreting neurons and the deposition of Lewy bodies formed by alpha-synuclein are found in PD, and these trigger motor symptoms, including slowness of movement, tremors, stiffness, and postural instability, as well as non-motor symptoms including cognitive changes, fatigue, mood disorders, and sleep disorders.^{28–32} A study by Guo et al. demonstrated that low-level expression of brain-derived neurotrophic factor antisense (BDNF-AS) protected neurons from A β _{25–35} neurotoxicity by enhancing cell viability and inhibiting apoptosis.³³ Meanwhile, in MPTP-induced PD models, a low expression of BDNF-AS may improve cell viability and suppress autophagy and apoptosis in the SH-SY5Y cell line by modulating miR-125b-5p.³⁴ However, the link between BDNF-AS and miR-125b-5p in the pathological processes of AD remains unknown.

Objectives

The current study aims to confirm the involvement of BDNF-AS and miR-125b-5p in the pathogenesis of AD, focusing on inflammation and apoptosis. The influence of BDNF-AS and miR-125b-5p on spatial learning and long-term memory was assessed by constructing AD rat models and conducting Morris water maze experiments. The effects on inflammation and apoptosis were studied at both the animal and cellular levels using AD rat tissues and AD cell models.

Materials and methods

Animal model

A total of 120 male Sprague Dawley rats of specific pathogen-free rank were obtained from the Shanghai Laboratory Animal Center at the Chinese Academy of Sciences (Shanghai, China) at the age of 8–12 weeks, weighing 22–30 g. The rats were raised in a standard environment with a 21–22°C temperature, 60–70% relative humidity, natural light, and free access to food and drink. The rats had 1 week to acclimatize to the conditions. The animals

were randomly assigned to one of 6 groups: sham, AD, AD+siRNA-negative control (si-NC), AD+si-BDNF-AS, AD+miR-NC, and AD+miR-125b-5p.

The AD rat model was constructed using human A β_{1-42} peptide. With the use of phosphate-buffered saline (PBS), A β_{1-42} peptides were dissolved at a concentration of 1 μ g/ μ L, and the solution was incubated at 37°C for 1 week to generate A β aggregation. The prepared A β_{1-42} solution (10 μ L/rat) or PBS (3 μ L/rat) was administered into the brain ventricles through stereotactic injection using a Hamilton microsyringe (designated coordinates: anteroposterior = 0.2 mm, mediolateral = 1.0 mm and dorsoventral = 2.5 mm) under anesthesia. A week after the A β_{1-42} injection, si-NC, si-BDNF-AS, miR-NC, and miR-125b-5p mimics were injected into the tail vein of the rats in the corresponding group. The tail vein of the rats in the sham group or AD group received an injection of PBS. All the experiments met the requirements of Shanghai Eighth People's Hospital's Ethics Committee (approval No. 2021-0510) for animal experiments.

Morris water maze

The Morris water maze experiment is used to measure spatial learning and memory in AD models.^{35,36} This test is divided into 2 sections: place navigation and spatial probing. A circular pool (diameter: 120 cm) was full of water, with a depth of 35 cm and at a temperature of 22–25°C, and an escape platform (diameter: 9 cm) was immersed approx. 1 cm below the surface of the water. Rats were individually trained 3 times a day for 7 days after the animal model was generated, and every time the rat was put in the water at different starting points. Each experiment lasted 90 s unless the rat touched the platform, and the time of first reaching the platform (escape latency) was recorded. In the probe trial (day 9), the rat had 90 s to search for the escape platform that had been removed. The amount of time the rat spent in the target quadrant, the previous location of the platform, and the number of times the rat crossed the platform location were recorded.

Primary cerebral cortex neuron culture and PC12 cell culture

As previously stated, the primary cerebral cortex neurons were isolated from the rat embryos (embryonic day 18 (E18)).³⁷ To separate cells, the cerebral cortex was taken from the E18 rat embryos, treated with papain (10 U/mL) for 10 min and rinsed with Dulbecco's modified Eagle medium (DMEM) containing 10% PBS. Neurons were plated at 1×10^5 cells/mL on a poly-L-lysine-coated dish with a neurobasal medium containing B27 supplement, penicillin, streptomycin, insulin, and L-glutamine. The cells were cultured in a B27-supplemented neurobasal medium (Gibco, Waltham, USA). The PC12 cells

were cultured in DMEM with 5% horse serum and 10% fetal bovine serum (FBS; Gibco). Additionally, 100 ng/mL of nerve growth factor (NGF) (Sigma-Aldrich, St. Louis, USA) was added to the medium of the PC12 cells to induce neuronal differentiation. All cells were grown in a humidified atmosphere with 5% CO₂ at 37°C.

Primary cerebral cortex neurons (NEU) and PC12 cells, stimulated by NGF, were cultured with different proportions of aggregated A β_{1-42} (0, 10, 20, and 40 μ M) for 24 h to test cell viability.

Reverse transcription-quantitative polymerase chain reaction (RT-qPCR)

Total RNAs were separated from rat serum or cell samples using TRIzol Reagent (Invitrogen, Waltham, USA) and quantified using Nanodrop (Thermo Fisher Scientific, Waltham, USA). The PrimeScript™ RT Reagent Kit (Takara, Kusatsu, Japan) was then implemented to reverse transcribe RNA into complementary DNA. The PCR conditions were 95°C for 5 min, followed by 40 cycles of 95°C for 5 s and 60°C for 30 s. The RT-qPCR findings were quantified using the 2^{−ΔΔCt} method with U6 or GAPDH as an internal reference.³⁸ The primers were generated by Sangon Biotech Co., Ltd. (Shanghai, China) and are listed in Supplementary Table 1.

Western blot

Total protein samples were extracted from the tissues or cells of each group using radioimmunoprecipitation assay (RIPA) lysis buffer (Sigma-Aldrich), and protein quantification was performed with a bicinchoninic acid (BCA) assay kit (Pierce Biotechnology, Waltham, USA). Protein samples (20 μ g) underwent electrophoresis in a 15% sodium dodecyl sulfate-polyacrylamide gel electrophoresis (SDS-PAGE) before being transferred to polyvinylidene fluoride (PVDF) membranes (Millipore, Burlington, USA). After 2 h of blocking with 5% non-fat milk, the membranes were incubated with the matching primary antibody at 4°C overnight. Then, they were incubated for 2 h at room temperature with horseradish peroxidase (HRP)-conjugated goat anti-mouse or goat anti-rabbit immunoglobulin G (IgG) as secondary antibodies. The ECL Chemiluminescent Substrate Reagent Kit (Invitrogen) was used to visualize the protein. The used rabbit monoclonal or polyclonal primary antibodies were as follows: Bcl-2 (1:2000, ab182858; Abcam, Cambridge, UK), Bax (1:1000, ab32503; Abcam), cleaved caspase-3 (1:500, ab2302; Abcam), TLR3 (1:3000, ab137722; Abcam), TLR4 (1:300, ab217274; Abcam), MyD88 (1:2000, ab133739; Abcam), TRIF (1:1000, #4596; Cell Signaling Technology, Danvers, USA), NF- κ B p65 (1:5000, ab32536; Abcam), and GAPDH (1:2500, ab9485; Abcam). Goat anti-rabbit IgG H&L (1:2000, ab6721; Abcam) was used as a secondary antibody.

MTT assay

The Cell Proliferation Reagent Kit I (3-(4,5-dimethylthiazol-2-yl)-2,5 diphenyl tetrazolium bromide (MTT)) (Sigma-Aldrich) was used to determine cell proliferation according to the manufacturer's protocol. Following suitable transfections, the 2 cell lines were maintained in 96-well plates. Each well received a total of 20 μ L of MTT solution (concentration: 5 mg/mL) and was treated in darkness for 4 h at 37°C. Then, 150 μ L of dimethyl sulfoxide (DMSO) was added to each well to dissolve the blue crystals. Finally, the absorbance value of each well was assessed on a microplate reader at 450 nm.

Cell apoptosis assay

The Annexin V-FITC kit (BD Biosciences, Franklin Lakes, USA) was used to assess cell apoptosis. After the transfection for 48 h, the 2 cell lines at a concentration of 1×10^6 /mL were collected and resuspended. Then, the cells were treated with 200 μ L of Annexin V-FITC for 10 min, after which propidium iodide (PI) was added to the mixture. Finally, flow cytometry (BD Biosciences) was used to determine the cell apoptosis rate.

Enzyme-linked immunosorbent assay

Using an enzyme-linked immunosorbent assay (ELISA) kit and following the manufacturer's instructions, the expression of interleukin 6 (IL-6), interleukin-1 β (IL-1 β) and tumor necrosis factor alpha (TNF- α) in tissues or cell supernatant was assessed.

Cell transfection

Small interfering RNA (siRNA) was synthesized by GenePharma (Shanghai, China). The 2 cell lines were transfected with si-NC, si-BDNF-AS, miR-NC, and miR-125b-5p mimic, according to the manufacturer's guidelines for Lipofectamine™ 3000 (Invitrogen).

Luciferase reporter assay

StarBase 3.0 (<http://starbase.sysu.edu.cn/>) was utilized to evaluate the targeted sites for potential interactions between *BDNF-AS* and *miR-125b-5p*. Full-length sequences and fragments of *BDNF-AS* that contained the potential binding site for *miR-125b-5p* were cloned into the pmir-GLO vector (Promega, Madison, USA). The 2 cell lines were co-transfected with the luciferase reporters, along with the miR-125b-5p mimic and the miR-NC. After 48 h, relative luciferase activity was measured using the Dual-Luciferase® Reporter Assay System (Promega).

Statistical analyses

The statistical analyses were conducted using IBM Statistical Package for Social Sciences (SPSS) v. 26.0 software (IBM Corp., Armonk, USA), with data presented as mean \pm standard deviation ($M \pm SD$). To confirm normality, we employed the Shapiro–Wilk test, while Levene's test was used to check the homogeneity of variance (Supplementary Tables 2 and 3 present the statistical results). Student's t-test was used to compare data from 2 groups for normally distributed and homogenous data, while one-way analysis of variance (ANOVA) followed by Tukey's post hoc test was applied to analyze 3 or more groups (Supplementary Tables 4 and 5 present the statistical results). In cases where the data were non-normal or violated homogeneity, or for small sample sizes (such as $n = 3$), we used the Mann–Whitney (M–W) U test for 2-group data analysis and Kruskal–Wallis (K–W) test followed by Dunn's post hoc test for analyzing 3 or more groups (Supplementary Table 6 presents the statistical results). Repeated measures ANOVA (RM ANOVA) followed by Tukey's post hoc test were used for analyzing the data related to escape distance and escape latency. A p-value of less than 0.05 was deemed statistically significant.

Results

Effects of lncRNA BDNF-AS and miR-125b-5p on spatial learning and long-term memory in the AD rat model

Repeated measures ANOVA demonstrated that escape distance and escape latency over 5 days varied substantially across groups in the Morris water maze experiment ($F = 14.29$, degrees of freedom (df) = 20, $p < 0.001$; $F = 22.69$, df = 20, $p < 0.001$). The experiment also revealed that the swimming distance and escape latency of rats in the sham group became shorter as the number of training days increased, indicating that the rats had gradually acquired the ability to find a platform during training (Fig. 1A,B). Compared to the sham group, rats in the AD group displayed considerably greater swimming distance and escape latency ($p < 0.001$). Compared to the control groups, the addition of si-BDNF-AS and miR-125b-5p mimics shortened the swimming distance and escape latency by improving the learning ability and memory of rats (both $p < 0.001$). On day 9, a probe test was performed to measure the time spent in the target area in order to test memory maintenance. The AD group spent substantially less time in the target quadrant than the sham group ($p < 0.001$), and the time values for the AD+si-BDNF-AS and AD+miR-125b-5p mimic groups were longer than for their respective control groups (both $p < 0.001$) (Fig. 1C). The above findings indicate that reduced expression of BDNF-AS and higher expression of miR-125b-5p mitigated the learning and memory impairment in the AD rat model caused by the injection of A β_{1-42} .

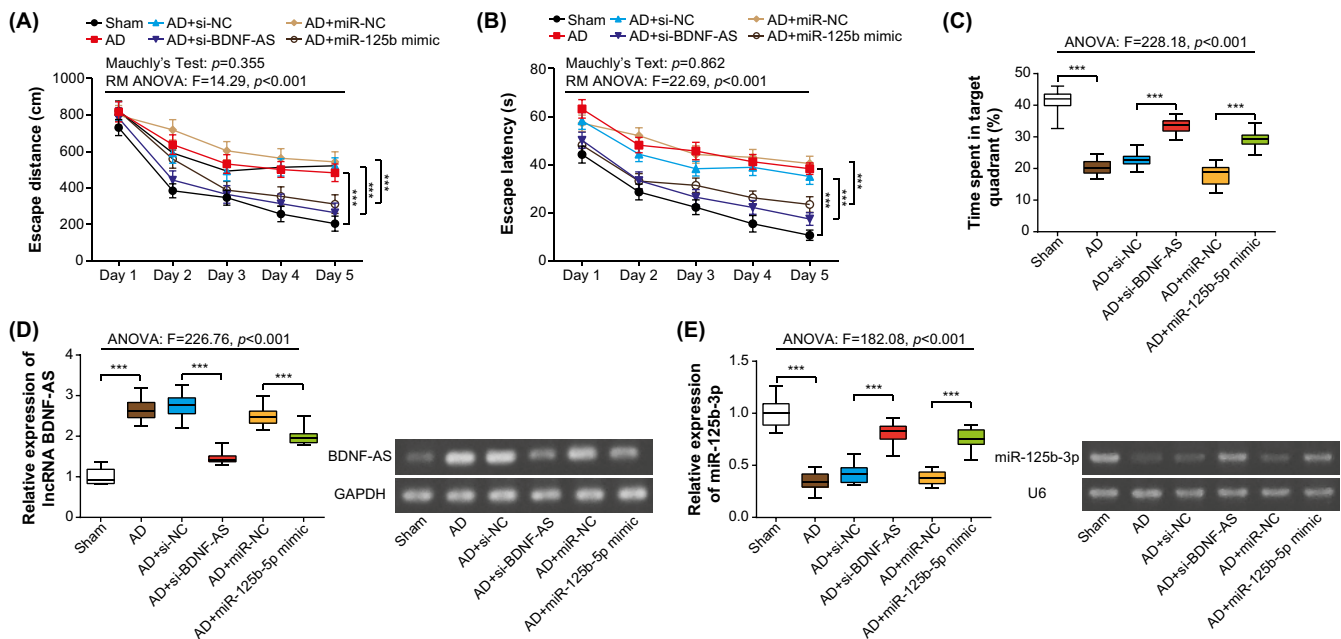


Fig. 1. Effects of lncRNA brain-derived neurotrophic factor antisense (BDNF-AS) and miR-125b-5p on memory impairment in the amyloid- β ($A\beta$)₁₋₄₂-treated Alzheimer's disease (AD) rat model. Escape distance (A) and latency (B) to arrive at the platform, as well as the amount of time (C) spent in the target quadrant and site within 60 s were automatically recorded. The expression levels of BDNF-AS (D) and miR-125b-5p (E) were examined in the sham, AD, AD+si-NC, AD+si-BDNF-AS, AD+miR-NC, and AD+miR-125b-5p mimic groups. A,B. *** $p < 0.001$ (Tukey's post hoc test following repeated measures analysis of variance (RM ANOVA)); C-E. *** $p < 0.001$ (Tukey's post hoc test following ANOVA). Data are presented using the median value as the middle line, with the 25th to 75th percentiles represented by the box. The minimum and maximum values are indicated with whiskers

Effects of lncRNA BDNF-AS and miR-125b-5p on the expression of BDNF-AS and miR-125b-5p in the AD rat model

We discovered that the expression level of BDNF-AS was 2.66 times greater in the AD group than in the sham group through the detection in the rat serum, while the expression level of miR-125b-5p was only 35% of the sham group's level (both $p < 0.001$) (Fig. 1D,E). The low-level expression of BDNF-AS and high-level expression of miR-125b-5p had a significant adverse effect on the expression levels of the 2 RNAs, when compared with their corresponding control groups (both $p < 0.001$) (Fig. 1D,E).

Effects of lncRNA BDNF-AS and miR-125b-5p on apoptosis in the AD rat model

The hippocampus tissue from the AD group showed a higher rate of apoptosis compared to the sham group ($p < 0.001$) (Fig. 2A). In the AD+si-BDNF-AS and AD+miR-125b-5p mimic groups, the apoptosis rate was effectively suppressed, and the apoptosis rate in these 2 groups was only 60.38–72.62% of that of their corresponding control group (both $p < 0.001$). At the same time, the levels of expression of apoptosis-related proteins differed among the groups ($F(5,114) = 283.60$, $p < 0.001$; $F(5,114) = 96.94$, $p < 0.001$; $F(5,114) = 94.06$, $p < 0.001$). The AD group had higher levels of Bax and cleaved caspase-3 and lower levels of Bcl-2 when compared with the sham group (both $p < 0.001$) (Fig. 2B). However,

compared with the respective control groups, the low-level expression of BDNF-AS and high-level expression of miR-125b-5p were able to successfully reduce Bax and cleaved caspase-3 expression while increasing Bcl-2 expression (both $p < 0.001$).

Effects of lncRNA BDNF-AS and miR-125b-5p on inflammation and inflammatory pathway-related proteins in the AD rat model

In terms of inflammatory factors, the AD group released higher levels of IL-1 β , IL-6 and TNF- α than the sham group (both $p < 0.001$) (Fig. 3A). Conversely, these levels were considerably suppressed in the AD+si-BDNF-AS and AD+miR-125b-5p mimic groups when compared to the control groups (both $p < 0.001$). The expression levels of TLR3, TLR4, MyD88, TRIF, and NF- κ B p65 were significantly increased in the AD group, and were 1.83–3.15 times higher than that of the sham group (both $p < 0.001$) (Fig. 3B,C). Compared to the corresponding control groups, adding si-BDNF-AS or miR-125b-5p mimic inhibited the production of these proteins (both $p < 0.001$).

Construction of AD cellular models

The MTT results revealed that in both the NGF-PC12 cells and primary cerebral cortex neurons, cell viability was considerably reduced in the $A\beta$ ₁₋₄₂ treated group compared to the NC group, which reflects the cytotoxic effect

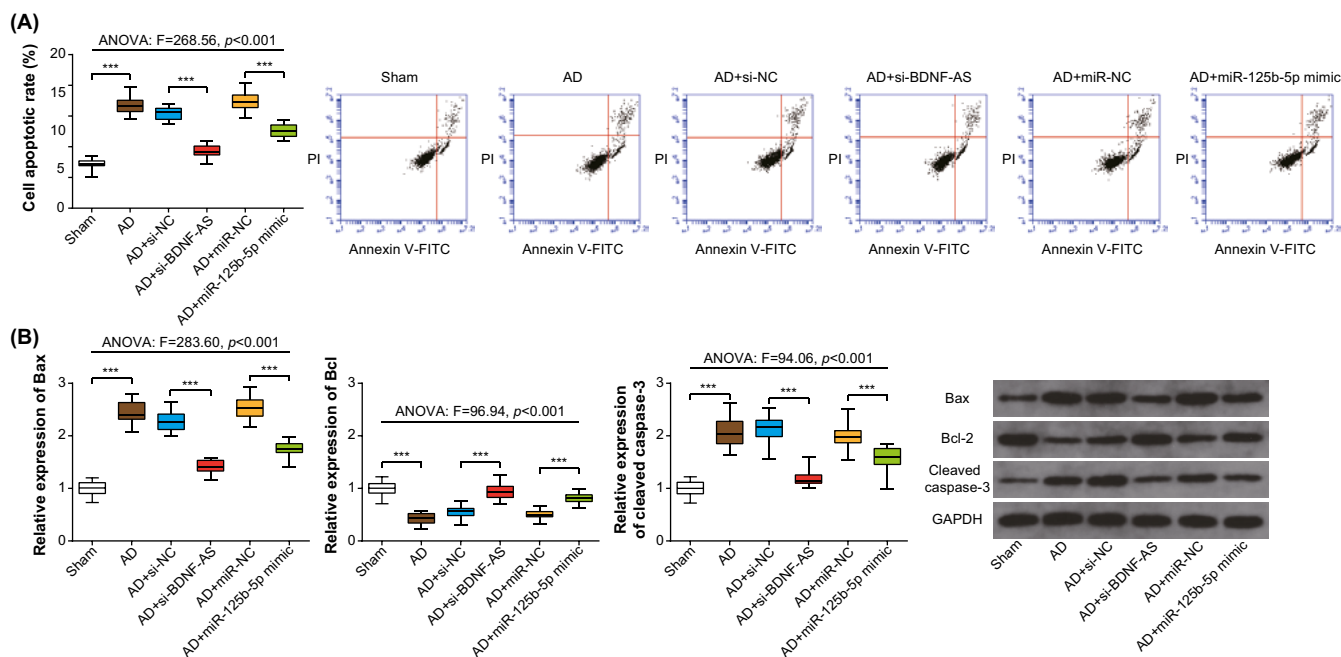


Fig. 2. Effects of lncRNA brain-derived neurotrophic factor antisense (BDNF-AS) and miR-125b-5p on apoptosis in the amyloid- β ($A\beta$)₁₋₄₂-treated Alzheimer's disease (AD) rat model. A, B. *** $p < 0.001$ (Tukey's post hoc test following analysis of variance (ANOVA)). Data are presented using the median value as the middle line, with the 25th to 75th percentiles represented by the box. The minimum and maximum values are indicated with whiskers

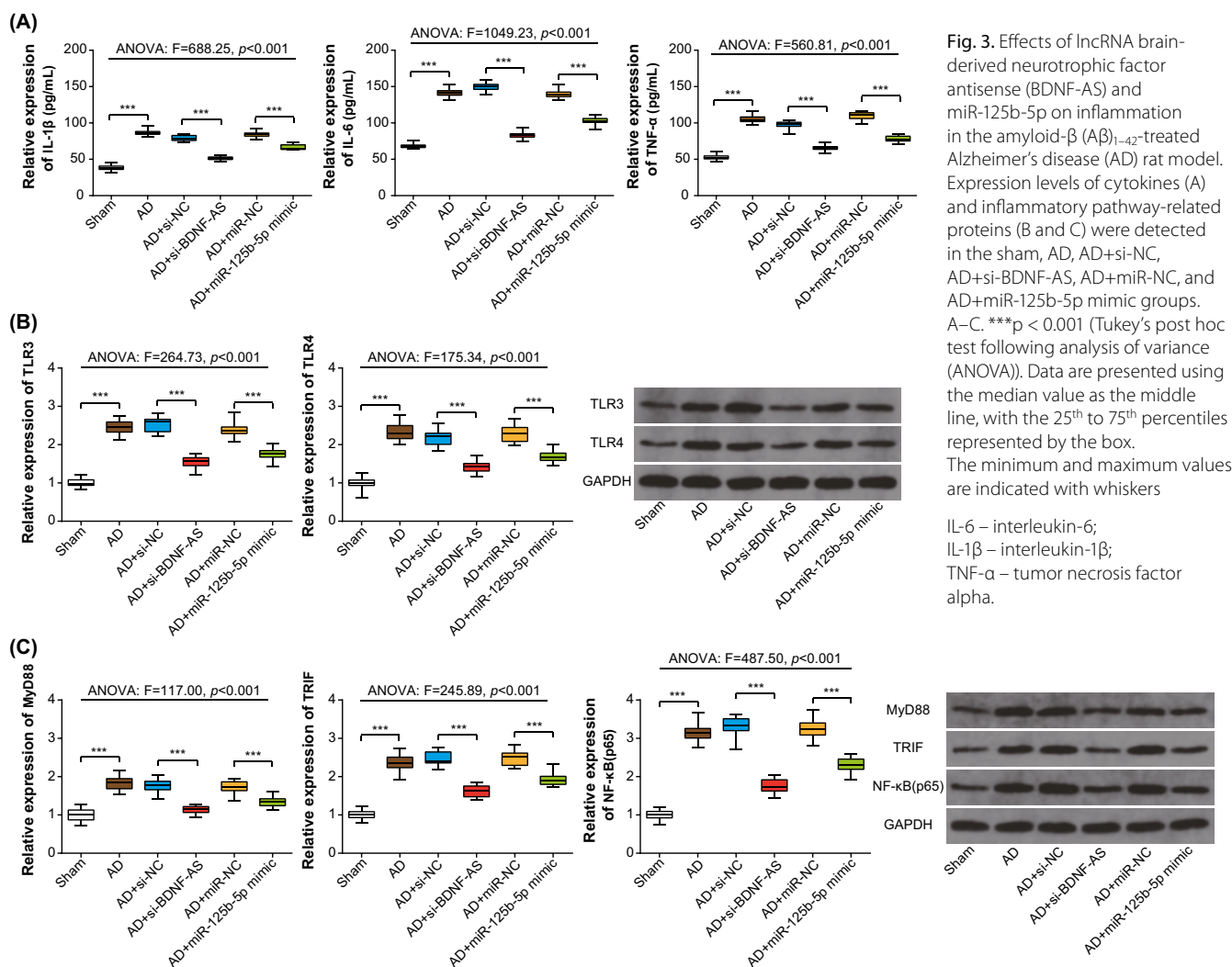


Fig. 3. Effects of lncRNA brain-derived neurotrophic factor antisense (BDNF-AS) and miR-125b-5p on inflammation in the amyloid- β ($A\beta$)₁₋₄₂-treated Alzheimer's disease (AD) rat model. Expression levels of cytokines (A) and inflammatory pathway-related proteins (B and C) were detected in the sham, AD, AD+si-NC, AD+si-BDNF-AS, AD+miR-NC, and AD+miR-125b-5p mimic groups. A–C. *** $p < 0.001$ (Tukey's post hoc test following analysis of variance (ANOVA)). Data are presented using the median value as the middle line, with the 25th to 75th percentiles represented by the box. The minimum and maximum values are indicated with whiskers

IL-6 – interleukin-6;
IL-1 β – interleukin-1 β ;
TNF- α – tumor necrosis factor alpha.

of A β_{1-42} , as well as a gradual decrease in cell viability with increasing concentrations of A β_{1-42} , and reflects the existence of a dose-dependent effect (K–W: $H = 9.97$, $p = 0.019$; $H = 10.39$, $p = 0.016$) (Fig. 4A). The above results confirmed the successful construction of 2 AD cellular models. Meanwhile, with an increase in A β_{1-42} concentration, the expression level of BDNF-AS increased and miR-125b-5p level decreased (K–W: $H = 10.39$, $p = 0.016$) (Fig. 4B,C). The NGF-PC12 cells and primary cerebral cortex neurons were treated with a 20- μ M dose of A β_{1-42} for 24 h to construct 2 AD cellular models for the following experiments.

After the transfection with si-BDNF-AS, the expression level of BDNF-AS was notably reduced compared to the NC group, while the addition of miR-125b-5p mimic promoted the expression of miR-125b-5p in both cellular models of AD (M–W U: $Z = -2.12$, $p = 0.034$) (Fig. 4D,E), reflecting successful transfections.

Effects of lncRNA BDNF-AS and miR-125b-5p on cell apoptosis in the cellular models of AD

In the 2 cellular models of AD, A β_{1-42} was capable of significantly elevating the rate of apoptosis compared to the NC group (PC12 cell: $p < 0.05$; NEU: $p < 0.005$). However, both low-level expression of BDNF-AS and high-level expression of miR-125b-5p were effective in inhibiting apoptosis induced by A β_{1-42} (both $p < 0.05$) (Fig. 5A). Western blot results for apoptotic-related proteins revealed that the expression of Bax and cleaved caspase-3 were reportedly elevated, while the expression of Bcl-2 was dramatically lowered in the A β_{1-42} group compared to the NC group (both $p < 0.05$) (Fig. 5B). However, the treatment with si-BDNF-AS or miR-125b-5p mimic suppressed the levels of Bax and cleaved caspase-3, and elevated the level of Bcl-2 compared to the corresponding control groups (both $p < 0.05$).

Effects of lncRNA BDNF-AS and miR-125b-5p on inflammation and inflammatory pathway-related proteins in the cellular models of AD

The ELISA results showed that the A β_{1-42} group secreted higher IL-1 β , IL-6 and TNF- α levels than the NC group (both $p < 0.05$) (Fig. 6A), while lower expression levels of inflammatory factors were detected in the A β_{1-42} +si-BDNF-AS or A β_{1-42} +miR-125b-5p mimic groups compared to the A β_{1-42} +si-NC or A β_{1-42} +miR-NC groups (both $p < 0.05$).

In contrast, the treatment with A β_{1-42} promoted the expression levels of TLR3, TLR4, MyD88, TRIF, and NF- κ B p65 in the 2 AD cellular models significantly more than in the NC group (both $p < 0.05$) (Fig. 6B,C). Both low-level expression of BDNF-AS and high-level expression of miR-125b-5p inhibited the promotion of inflammatory pathway-related proteins stimulated by A β_{1-42} (both $p < 0.05$).

miR-125b-5p is the target gene of lncRNA BDNF-AS

The binding location for lncRNA BDNF-AS and miR-125b-5p was predicted using StarBase 3.0 (<http://starbase.sysu.edu.cn/>) (Fig. 7A). The luciferase activity in 2 AD cellular models was lowered in the pmirGLO-BDNF-AS-Wt+miR-125b-5p mimic group when compared to the pmirGLO-BDNF-AS-Wt+miR-NC group (M–W U: $Z = -2.12$, $p = 0.034$) (Fig. 7A). Furthermore, the expression of miR-125b-5p was considerably higher in the si-BDNF-AS group compared to the NC group (PC12 cell: U: $Z = -2.14$, $p = 0.032$; NEU: U: $Z = -2.12$, $p = 0.034$) (Fig. 7B).

Discussion

This study demonstrated that lncRNA BDNF-AS was substantially upregulated, and miR-125b-3p was decreased in an AD rat model. In addition, decreasing expression of BDNF-AS inhibited neuronal apoptosis, inflammation and inflammatory pathway-related proteins. Further evidence revealed that the knockdown of BDNF-AS could exert a neuroprotective effect by targeting miR-125b-5p.

A massive loss of neurons is one of the characteristic pathological changes in AD, especially in the cortex, hippocampus, and other brain areas related to learning and memory, and is closely associated with the onset of impairments in memory and cognition.^{39,40} The A β can change the Bcl-2/Bax ratio and activate caspase-3, triggering a downstream apoptotic cascade, promoting reactive oxygen species (ROS) accumulation, and resulting in cell death.⁴¹ In the study by Chu et al., the caspase family was shown to directly participate in the cleavage of A β and, after being cleaved by caspase-3, the A β with an abnormal C-terminal had a cytotoxic effect that could induce cell apoptosis.⁴² Meanwhile, caspase-3 is also involved in the cleavage of tau protein into truncated amino acid fragments, 19 of which are effectors of cell apoptosis. Moreover, caspase-3 is related to the cleavage of PS-1 and PS-2, which promotes the hydrolysis of amyloid precursor protein (APP) to release more A β and leads to neuronal apoptosis.

The above results are consistent with the present study demonstrating that cell apoptotic rates were promoted after A β treatment in the rat and cell models, and this promotion could be inhibited by si-BDNF-AS and miR-125b5p mimics (Fig. 2A, Fig. 5A). The knockdown of BDNF-AS has been shown to increase the mitochondrial membrane potential and prevent the release of cytochrome c from the mitochondria.⁴³ Therefore, the Bcl-2/Bax ratio, caspase-3 activation and apoptotic rate were reversed due to the effect of BDNF-AS siRNA on protection against mitochondrial damage. While miR-125b-5p regulates the synaptic protein synapsin-2 (SYN-2) and 15-lipoxygenase (15-LOX), it causes synaptic and neurotrophic deficits that are linked to neuronal apoptosis.^{44,45}

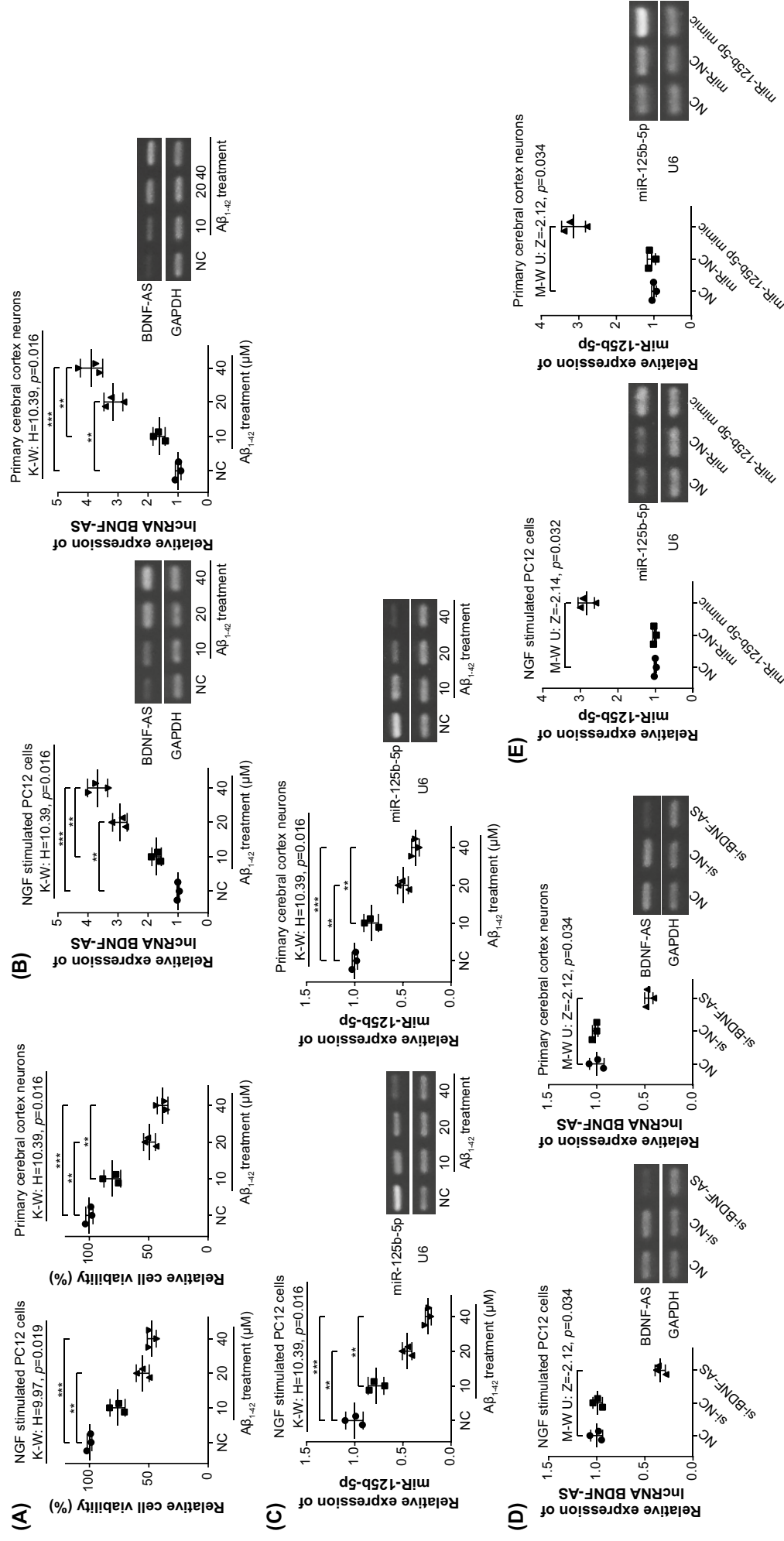


Fig. 4. Construction of cellular models of Alzheimer's disease (AD). The cell viabilities of nerve growth factor (NGF)-stimulated PC12 cells and primary cerebral cortex neurons were monitored after treatment with amyloid- β (A β)₁₋₄₂ at different concentrations (A). The expression levels of brain-derived neurotrophic factor antisense (BDNF-AS) (B) and miR-125b-5p (C) were determined after the treatment with A β ₁₋₄₂ at different concentrations. After transfection of si-NC and si-BDNF-AS, the expression level of lncRNA BDNF-AS was evaluated (D). The level of miR-125b-5p expression was determined in the NC, miR-NC and miR-125b-5p mimic groups (E). A-C. ***p < 0.005 (Dunn's post hoc test following Kruskal-Wallis (K-W) test), and **p < 0.05 (Dunn's post hoc test following K-W test); D-E. The results were statistically analyzed using the Mann-Whitney (M-W) U test. Data are presented as median with range

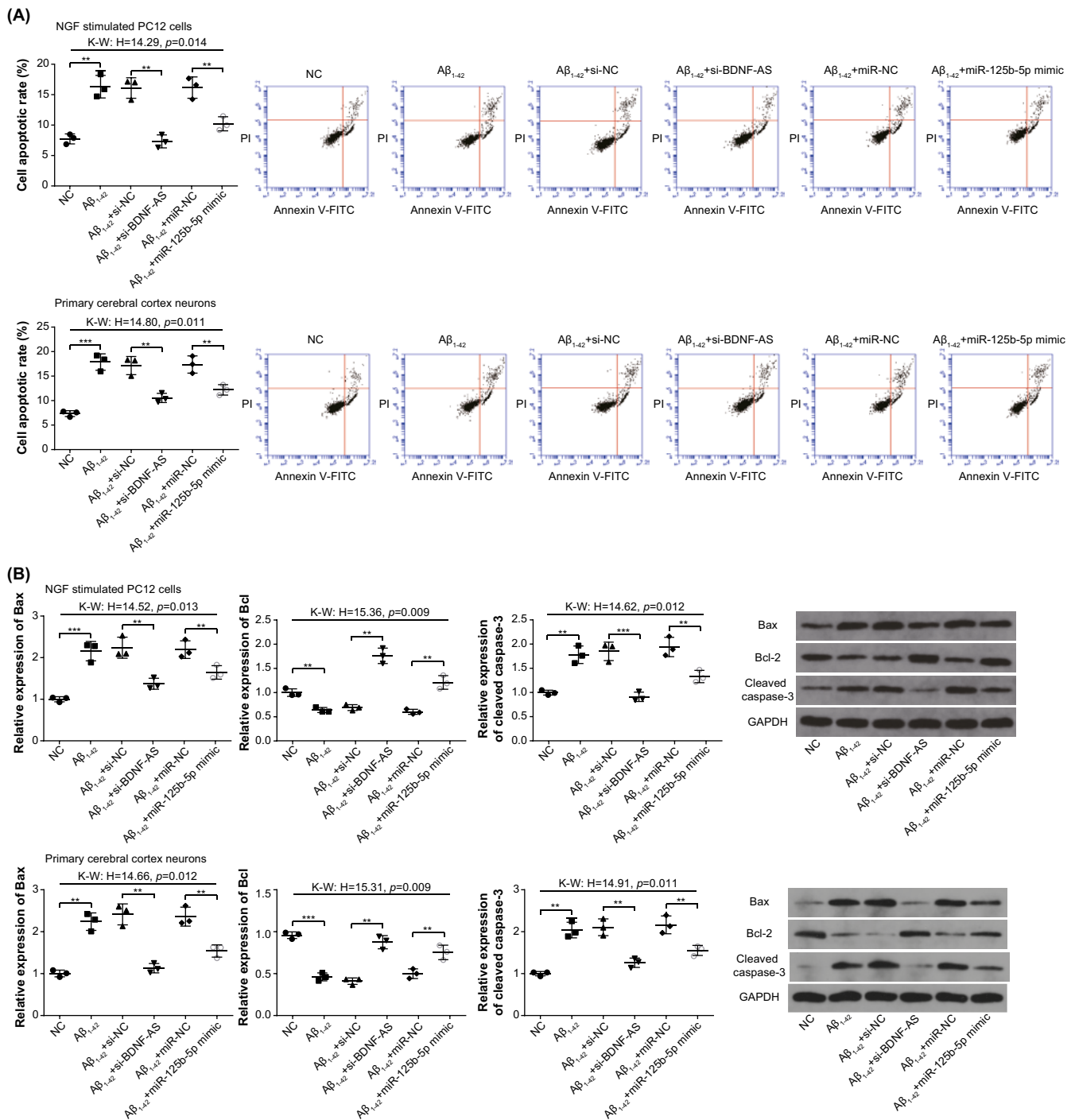


Fig. 5. Effects of lncRNA brain-derived neurotrophic factor antisense (BDNF-AS) and miR-125b-5p on apoptosis in the 2 cellular Alzheimer's disease (AD) models. Cell apoptosis rate (A) and apoptotic-related proteins (B) were detected in the NC, amyloid- β ($A\beta$) $_{1-42}$, $A\beta_{1-42} + \text{si-NC}$, $A\beta_{1-42} + \text{si-BDNF-AS}$, $A\beta_{1-42} + \text{miR-NC}$, and $A\beta_{1-42} + \text{miR-125b-5p mimic}$ groups. A,B. *** $p < 0.005$ (Dunn's post hoc test following Kruskal–Wallis (K–W) test); ** $p < 0.05$ (Dunn's post hoc test following K–W test). Data are presented as median with range

NGF – nerve growth factor.

In the process of AD, $A\beta$ deposition and abnormal phosphorylation of tau protein are the main mechanisms leading to microglial inflammation.^{46,47} The $A\beta$ can be recognized by complement receptors and cytokine receptors on the membranes of microglia and astrocytes, thereby promoting the synthesis and secretion of inflammatory factors such as ROS, TNF- α , IL-1 β , and IL-6.⁴⁸ As shown in Fig. 3A and Fig. 6A, elevated expression of TNF- α , IL-1 β , and IL-6

was found after stimulation of $A\beta$. Continuous microglial activation and the release of inflammatory factors can aggravate neuronal damage and lead to exacerbated NFTs.⁴⁹ At the same time, this process can decrease the ability of microglia to clear $A\beta$, raise the levels of $A\beta$, and aggravate pathological damage. On the other hand, $A\beta$ can directly activate TLRs to cause microglia-mediated inflammation.⁵⁰ Studies have found that in the AD model, the expression levels

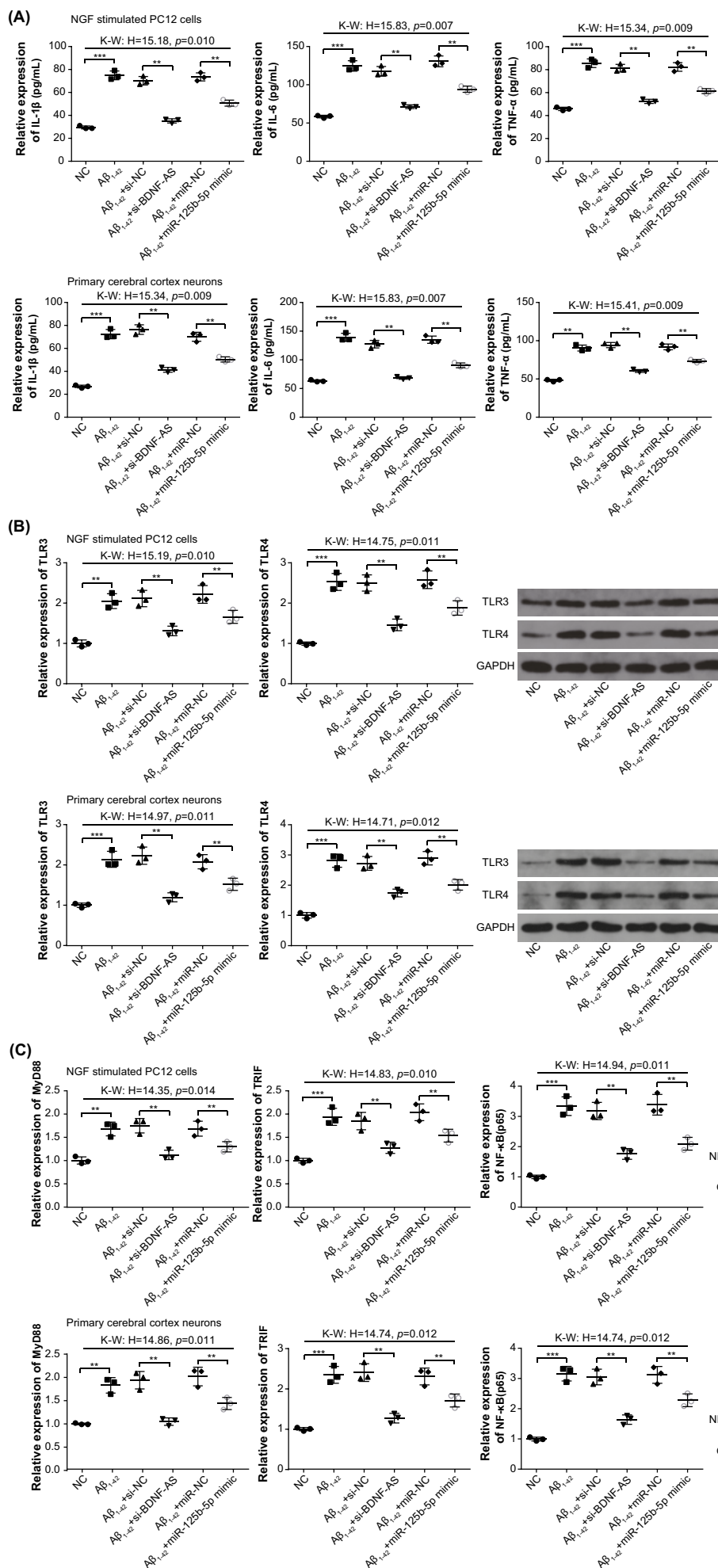


Fig. 6. Effects of lncRNA brain-derived neurotrophic factor antisense (BDNF-AS) and miR-125b-5p on inflammation in the 2 cellular Alzheimer's disease (AD) models. Expression levels of cytokines (A) and inflammatory pathway-related proteins (B,C) were evaluated in the NC, amyloid- β ($A\beta_{1-42}$), $A\beta_{1-42}$ +si-NC, $A\beta_{1-42}$ +si-BDNF-AS, $A\beta_{1-42}$ +miR-NC, and $A\beta_{1-42}$ +miR-125b-5p mimic groups. A-C. *** $p < 0.005$ (Dunn's post hoc test following Kruskal-Wallis (K-W) test); ** $p < 0.05$ (Dunn's post hoc test following K-W test). Data are presented as median with range

IL-6 – interleukin 6;
IL-1 β – interleukin 1 β ;
TNF- α – tumor necrosis factor alpha; NGF – nerve growth factor.

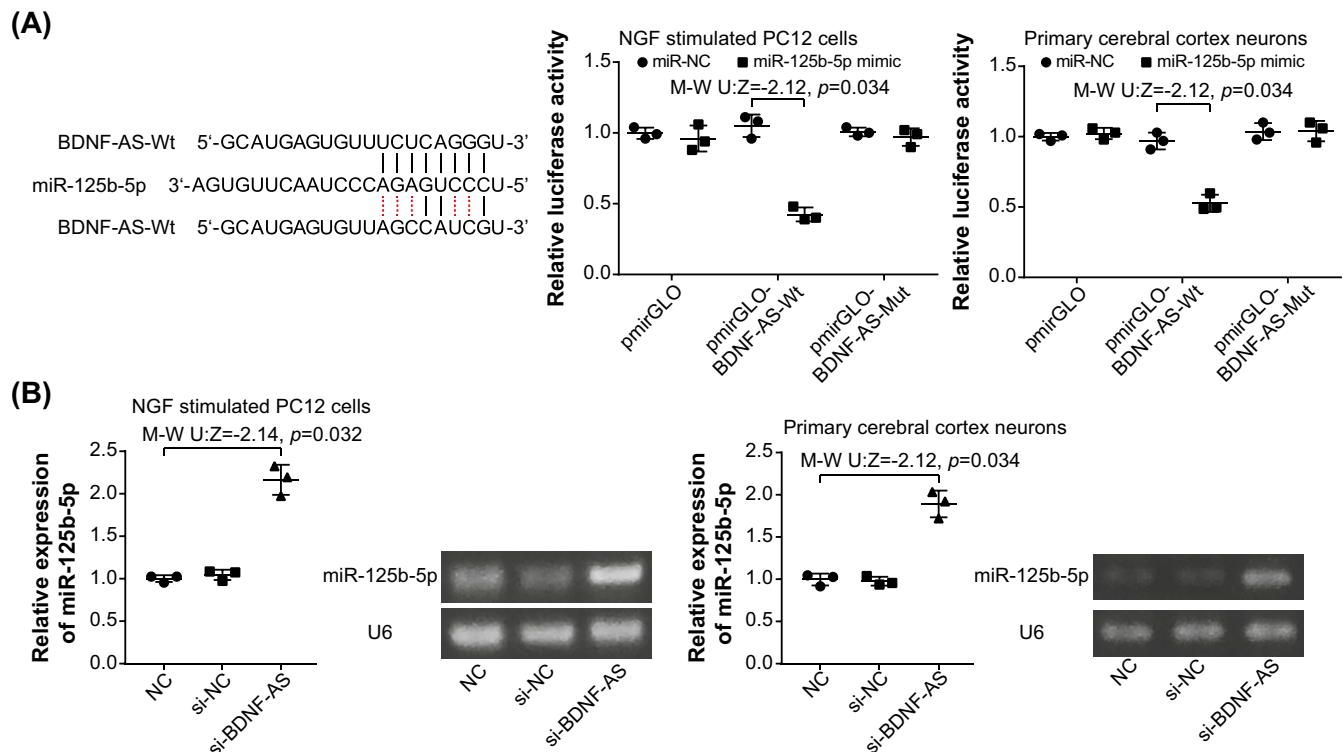


Fig. 7. *miR-125b-5p* is the target gene of the lncRNA brain-derived neurotrophic factor antisense (BDNF-AS). A. *miR-125b-5p* targeted BDNF-AS at specific sites, and luciferase activities were compared between groups of BDNF-AS-Wt+*miR-125b-5p* mimic, BDNF-AS-Wt+*miR-NC*, and BDNF-AS-Mut+*miR-125b-5p* mimic; B. *miR-125b-5p* expression was altered after si-BDNF-AS transfection. The results were statistically analyzed using the Mann–Whitney (M–W) U test. Data are presented as median with range

NGF – nerve growth factor.

of TLR3 and TLR4 are increased, and these may be the main subtypes of TLRs activated by A β .⁵¹ In the present study, the expression levels of TLR3, TLR4, MyD88, TRIF, and NF- κ B p65 were all increased in the A β group but were decreased in the A β _{1–42}+si-BDNF-AS or A β _{1–42}+*miR-125b-5p* mimic groups. Elevated TLR3 and TLR4 can trigger NF- κ B after activating the downstream signaling pathway by binding to MyD88 or TRIF.⁵²

As the most common cause of dementia, there are no specific, standard treatment options for AD, which is often diagnosed late and has a significant impact on a patient's quality of life.^{53,54} Compared to established diagnostic methods, such as structural MRI of the hippocampal and molecular neuroimaging utilizing positron emission tomography (PET), the detection of miRNAs in bodily fluids is a relatively simple procedure. The ability of prospective biomarkers to detect the disease at an early stage and track the development of brain function would be a significant contribution. Current drugs, such as donepezil, rivastigmine and galantamine, can temporarily relieve dementia symptoms, but cannot terminate the progression of the disease. The fact that miRNAs are implicated in amyloid peptide aggregates, hyperphosphorylated tau protein aggregation, synaptic loss, neuroinflammation, and defective autophagy favors the development of miRNA-based therapeutic strategies.⁵⁵

Limitations

Because of a limited budget, this study only focused on cell apoptosis and inflammation. Therefore, limited experiments were conducted on the AD rat and cellular models. The effects of BDNF-AS and *miR-125b-5p* on neurite outgrowth and oxidative stress are still unknown. Further exploration of the relationship between molecular regulation and neuropathological changes will be useful in future AD research.

Conclusions

To conclude, lncRNA BDNF-AS siRNA represses cell apoptosis and inflammation via targeting of *miR-125b-5p* in AD, which suggests a strong association between BDNF-AS and the pathological mechanism of AD. The investigation of BDNF-AS and its downstream targets helps to expand our understanding of BDNF as a key molecule involved in neuronal changes related to learning and memory, laying the groundwork for new biomarkers or promising therapeutic targets for AD treatment.

Supplementary data

The supplementary materials are available at <https://doi.org/10.5281/zenodo.7990783>. The package contains the following files:

Supplementary Table 1. Primer sequences used in RT-qPCR of this study.

Supplementary Table 2. The results of normality test in the AD rat model.

Supplementary Table 3. The results of Levene's test in the AD rat model.

Supplementary Table 4. The means and 95% CI of ANOVA in the AD rat model.

Supplementary Table 5. The results of ANOVA in the AD rat model.

Supplementary Table 6. The statistical analysis results of the AD cellular model.

ORCID iDs

Haiyan Ren  <https://orcid.org/0009-0007-7531-779X>
 Weibin Qiu  <https://orcid.org/0009-0009-0731-4399>
 Benju Zhu  <https://orcid.org/0009-0007-2455-5384>
 Qiang Li  <https://orcid.org/0009-0009-8978-0333>
 Chen Peng  <https://orcid.org/0009-0008-1807-4207>
 Xu Chen  <https://orcid.org/0000-0003-3465-6932>

References

- Sengoku R. Aging and Alzheimer's disease pathology. *Neuropathology*. 2020;40(1):22–29. doi:10.1111/neup.12626
- Gunn-Moore D, Kaidanovich-Beilin O, Iradi MCG, Gunn-Moore F, Lovestone S. Alzheimer's disease in humans and other animals: A consequence of postreproductive life span and longevity rather than aging. *Alzheimers Dement*. 2018;14(2):195–204. doi:10.1016/j.jalz.2017.08.014
- Dugger BN, Dickson DW. Pathology of neurodegenerative diseases. *Cold Spring Harb Perspect Biol*. 2017;9(7):a028035. doi:10.1101/cshperspect.a028035
- Tanaka M, Toldi J, Vécsei L. Exploring the etiological links behind neurodegenerative diseases: Inflammatory cytokines and bioactive kynurenines. *Int J Mol Sci*. 2020;21(7):2431. doi:10.3390/ijms21072431
- Hashimoto A, Matsuoka K, Yasuno F, et al. Frontal lobe function in elderly patients with Alzheimer's disease and caregiver burden. *Psychogeriatrics*. 2017;17(4):267–272. doi:10.1111/psyg.12231
- Dhikav V, Duraiswamy S, Anand KS. Correlation between hippocampal volumes and medial temporal lobe atrophy in patients with Alzheimer's disease. *Ann Indian Acad Neurol*. 2017;20(1):29–35. doi:10.4103/0972-2327.199903
- Rajmohan R, Reddy PH. Amyloid-beta and phosphorylated tau accumulations cause abnormalities at synapses of Alzheimer's disease neurons. *J Alzheimers Dis*. 2017;57(4):975–999. doi:10.3233/JAD-160612
- Battaglia S, Garofalo S, Di Pellegrino G. Context-dependent extinction of threat memories: Influences of healthy aging. *Sci Rep*. 2018;8(1):12592. doi:10.1038/s41598-018-31000-9
- Takahashi RH, Nagao T, Gouras GK. Plaque formation and the intraneuronal accumulation of β -amyloid in Alzheimer's disease. *Pathol Int*. 2017;67(4):185–193. doi:10.1111/pin.12520
- Battaglia S, Garofalo S, Di Pellegrino G, Starita F. Revaluing the role of vmPFC in the acquisition of Pavlovian threat conditioning in humans. *J Neurosci*. 2020;40(44):8491–8500. doi:10.1523/JNEUROSCI.0304-20.2020
- Nobakht M, Hoseini SM, Mortazavi P, et al. Neuropathological changes in brain cortex and hippocampus in a rat model of Alzheimer's disease. *Iran Biomed J*. 2011;15(1–2):51–58. PMID:21725500.
- Chen GF, Xu TH, Yan Y, et al. Amyloid beta: Structure, biology and structure-based therapeutic development. *Acta Pharmacol Sin*. 2017;38(9):1205–1235. doi:10.1038/aps.2017.28
- Sharma K, Pradhan S, Duffy LK, Yeasmin S, Bhattarai N, Schulte MK. Role of receptors in relation to plaques and tangles in Alzheimer's disease pathology. *Int J Mol Sci*. 2021;22(23):12987. doi:10.3390/ijms222312987
- Bloom GS. Amyloid- β and tau: The trigger and bullet in Alzheimer disease pathogenesis. *JAMA Neurol*. 2014;71(4):505–508. doi:10.1001/jamaneurol.2013.5847
- Iloside attenuate amyloid-beta pathology by reversing BDNF/TrkB signaling deficits and mitochondrial dysfunction. *Mol Neurobiol*. 2022;59(5):3091–3109. doi:10.1007/s12035-022-02728-3
- Harrison TM, Maass A, Adams JN, Du R, Baker SL, Jagust WJ. Tau deposition is associated with functional isolation of the hippocampus in aging. *Nat Commun*. 2019;10(1):4900. doi:10.1038/s41467-019-12921-z
- Liang SY, Wang ZT, Tan L, Yu JT. Tau toxicity in neurodegeneration. *Mol Neurobiol*. 2022;59(6):3617–3634. doi:10.1007/s12035-022-02809-3
- Wu M, Zhang M, Yin X, et al. The role of pathological tau in synaptic dysfunction in Alzheimer's diseases. *Transl Neurodegener*. 2021;10(1):45. doi:10.1186/s40035-021-00270-1
- Beylerli O, Gareev I, Sufianov A, Ilyasova T, Zhang F. The role of microRNA in the pathogenesis of glial brain tumors. *Noncoding RNA Res*. 2022;7(2):71–76. doi:10.1016/j.ncrna.2022.02.005
- Miya Shaik M, Tamargo I, Abubakar M, Kamal M, Greig N, Gan S. The role of microRNAs in Alzheimer's disease and their therapeutic potentials. *Genes (Basel)*. 2018;9(4):174. doi:10.3390/genes9040174
- O'Brien J, Hayder H, Zayed Y, Peng C. Overview of microRNA biogenesis, mechanisms of actions, and circulation. *Front Endocrinol (Lausanne)*. 2018;9:402. doi:10.3389/fendo.2018.00402
- Paul P, Chakraborty A, Sarkar D, et al. Interplay between miRNAs and human diseases. *J Cell Physiol*. 2018;233(3):2007–2018. doi:10.1002/jcp.25854
- Cardoso AL, Guedes JR. Quantifying miRNA deregulation in Alzheimer's disease. In: Perneczky R, ed. *Biomarkers for Alzheimer's Disease Drug Development*. Vol. 1750. Methods in Molecular Biology. New York, USA: Springer New York; 2018:307–319. doi:10.1007/978-1-4939-7704-8_21
- Chang WS, Wang YH, Zhu XT, Wu CJ. Genome-wide profiling of miRNA and mRNA expression in Alzheimer's disease. *Med Sci Monit*. 2017;23:2721–2731. doi:10.12659/MSM.905064
- Hou T, Zhou Y, Zhu L, et al. Correcting abnormalities in miR-124/PTPN1 signaling rescues tau pathology in Alzheimer's disease. *J Neurochem*. 2020;154(4):441–457. doi:10.1111/jnc.14961
- Ma Y, Ye J, Zhao L, Pan D. MicroRNA-146a inhibition promotes total neurite outgrowth and suppresses cell apoptosis, inflammation, and STAT1/MYC pathway in PC12 and cortical neuron cellular Alzheimer's disease models. *Braz J Med Biol Res*. 2021;54(5):e9665. doi:10.1590/1414-431x20209665
- Liu L, Liu L, Lu Y, Zhang T, Zhao W. Serum aberrant expression of miR-24-3p and its diagnostic value in Alzheimer's disease. *Biomark Med*. 2021;15(16):1499–1507. doi:10.2217/bmm-2021-0098
- Battaglia S, Thayer JF. Functional interplay between central and autonomic nervous systems in human fear conditioning. *Trends Neurosci*. 2022;45(7):504–506. doi:10.1016/j.tins.2022.04.003
- Battaglia S, Orsolini S, Borgomaneri S, Barbieri R, Diciotti S, Di Pellegrino G. Characterizing cardiac autonomic dynamics of fear learning in humans. *Psychophysiology*. 2022;59(12):e14122. doi:10.1111/psyp.14122
- Atik A, Stewart T, Zhang J. Alpha-synuclein as a biomarker for Parkinson's disease. *Brain Pathol*. 2016;26(3):410–418. doi:10.1111/bpa.12370
- Li KL, Huang HY, Ren H, Yang XL. Role of exosomes in the pathogenesis of inflammation in Parkinson's disease. *Neural Regen Res*. 2022;17(9):1898–1906. doi:10.4103/1673-5374.335143
- Ellena G, Battaglia S, Lădavas E. The spatial effect of fearful faces in the autonomic response. *Exp Brain Res*. 2020;238(9):2009–2018. doi:10.1007/s00221-020-05829-4
- Guo CC, Jiao CH, Gao ZM. Silencing of LncRNA BDNF-AS attenuates $A\beta_{25-35}$ -induced neurotoxicity in PC12 cells by suppressing cell apoptosis and oxidative stress. *Neuro Res*. 2018;40(9):795–804. doi:10.1080/01616412.2018.1480921
- Fan Y, Zhao X, Lu K, Cheng G. LncRNA BDNF-AS promotes autophagy and apoptosis in MPTP-induced Parkinson's disease via ablating microRNA-125b-5p. *Brain Res Bull*. 2020;157:119–127. doi:10.1016/j.brainresbull.2020.02.003

35. Hu J, Huang HZ, Wang X, et al. Activation of glycogen synthase kinase-3 mediates the olfactory deficit-induced hippocampal impairments. *Mol Neurobiol*. 2015;52(3):1601–1617. doi:10.1007/s12035-014-8953-9
36. Wang X, Wang LP, Tang H, et al. Acetyl-L-carnitine rescues scopolamine-induced memory deficits by restoring insulin-like growth factor II via decreasing p53 oxidation. *Neuropharmacology*. 2014;76(Pt A):80–87. doi:10.1016/j.neuropharm.2013.08.022
37. Kudoh SN, Kiyohara A, Taguchi T. The heterogeneous distribution of functional synaptic connections in rat hippocampal dissociated neuron cultures. *Electron Comm Jpn*. 2009;92(6):41–49. doi:10.1002/ecj.10063
38. Livak KJ, Schmittgen TD. Analysis of relative gene expression data using real-time quantitative PCR and the 2^{−(Delta Delta C(T))} method. *Methods*. 2001;25(4):402–408. doi:10.1006/meth.2001.1262
39. Kwon MJ, Kim S, Han MH, Lee SB. Epigenetic changes in neurodegenerative diseases. *Mol Cells*. 2016;39(11):783–789. doi:10.14348/molcells.2016.0233
40. Candini M, Battaglia S, Benassi M, Di Pellegrino G, Frassinetti F. The physiological correlates of interpersonal space. *Sci Rep*. 2021;11(1):2611. doi:10.1038/s41598-021-82223-2
41. Cui J, Shan R, Cao Y, Zhou Y, Liu C, Fan Y. Protective effects of ginsenoside Rg2 against memory impairment and neuronal death induced by Aβ_{25–35} in rats. *J Ethnopharmacol*. 2021;266:113466. doi:10.1016/j.jep.2020.113466
42. Chu J, Lauretti E, Praticò D. Caspase-3-dependent cleavage of Akt modulates tau phosphorylation via GSK3β kinase: Implications for Alzheimer's disease. *Mol Psychiatry*. 2017;22(7):1002–1008. doi:10.1038/mp.2016.214
43. Ebrahim K, Vatanpour H, Zare A, Shirazi FH, Nakhjavani M. Anticancer activity a of Caspian cobra (*Naja naja oxiana*) snake venom in human cancer cell lines via induction of apoptosis. *Iran J Pharm Res*. 2016;15(Suppl):101–112. PMID:28228809.
44. Basavaraju M, De Lencastre A. Alzheimer's disease: Presence and role of microRNAs. *Biomol Concepts*. 2016;7(4):241–252. doi:10.1515/bmc-2016-0014
45. Van den Hove DL, Kompotis K, Lardenoije R, et al. Epigenetically regulated microRNAs in Alzheimer's disease. *Neurobiol Aging*. 2014;35(4):731–745. doi:10.1016/j.neurobiolaging.2013.10.082
46. Anwar S, Rivest S. Alzheimer's disease: Microglia targets and their modulation to promote amyloid phagocytosis and mitigate neuroinflammation. *Expert Opin Ther Targets*. 2020;24(4):331–344. doi:10.1080/14728222.2020.1738391
47. Battaglia S. Neurobiological advances of learned fear in humans. *Adv Clin Exp Med*. 2022;31(3):217–221. doi:10.17219/acem/146756
48. Heppner FL, Ransohoff RM, Becher B. Immune attack: The role of inflammation in Alzheimer disease. *Nat Rev Neurosci*. 2015;16(6):358–372. doi:10.1038/nrn3880
49. Sung PS, Lin PY, Liu CH, Su HC, Tsai KJ. Neuroinflammation and neurogenesis in Alzheimer's disease and potential therapeutic approaches. *Int J Mol Sci*. 2020;21(3):701. doi:10.3390/ijms21030701
50. Abulfadl Y, El-Maraghy N, Ahmed AE, Nofal S, Abdel-Mottaleb Y, Badary O. Thymoquinone alleviates the experimentally induced Alzheimer's disease inflammation by modulation of TLRs signaling. *Hum Exp Toxicol*. 2018;37(10):1092–1104. doi:10.1177/0960327118755256
51. Mazarati A, Maroso M, Iori V, Vezzani A, Carli M. High-mobility group box-1 impairs memory in mice through both toll-like receptor 4 and Receptor for Advanced Glycation End Products. *Exp Neurol*. 2011;232(2):143–148. doi:10.1016/j.expneurol.2011.08.012
52. Zhao BS, Liu Y, Gao XY, Zhai HQ, Guo JY, Wang XY. Effects of ginsenoside Rg1 on the expression of toll-like receptor 3, 4 and their signalling transduction factors in the NG108-15 murine neuroglial cell line. *Molecules*. 2014;19(10):16925–16936. doi:10.3390/molecules191016925
53. Graham WV, Bonito-Oliva A, Sakmar TP. Update on Alzheimer's disease therapy and prevention strategies. *Annu Rev Med*. 2017;68:413–430. doi:10.1146/annurev-med-042915-103753
54. Valenza M, Scuderi C. How useful are biomarkers for the diagnosis of Alzheimer's disease and especially for its therapy? *Neural Regen Res*. 2022;17(10):2205–2207. doi:10.4103/1673-5374.335791
55. Walgrave H, Zhou L, De Strooper B, Salta E. The promise of microRNA-based therapies in Alzheimer's disease: Challenges and perspectives. *Mol Neurodegener*. 2021;16(1):76. doi:10.1186/s13024-021-00496-7